

## Deep-learning reconstruction of the prostate improves image quality and acquisition time in T2-weighted imaging

Daichi Kobayashi<sup>1</sup>, Hayato Tomita<sup>1</sup>, Tsuyoshi Morimoto<sup>1</sup>, Yuki Deguchi<sup>1</sup>, Hirofumi Fukuchi<sup>1</sup>, Hikaru Ishida<sup>1</sup>, Kumie Miyakawa<sup>1</sup>, Yasuyuki Kobayashi<sup>2</sup> and Hidefumi Mimura<sup>1</sup>

<sup>1</sup>Department of Radiology, St. Marianna University School of Medicine, Kawasaki, Japan

<sup>2</sup>Department of Advanced Biomedical Imaging Informatics, St. Marianna University School of Medicine, Kawasaki, Japan

### ABSTRACT

We compared the qualitative and quantitative quality of prostate conventional T2-weighted imaging and T2-weighted imaging with deep-learning reconstruction. Patients with suspected prostate cancer undergoing magnetic resonance imaging between April 2022 and June 2023 were included. Quantitative analysis was performed to determine the signal-to-noise and contrast ratios of the perirectal fat tissue, internal obturator muscle, and pubic tubercle. Eight periprostatic anatomical structures, overall image quality, and motion artifacts were evaluated by two radiologists using 5- or 4-point scales. Qualitative analysis results were compared to determine the agreement between the two radiologists. In total, 106 patients (mean age: 71 ± 8.3 years; 106 men) were included in this study. The acquisition time for conventional T2-weighted imaging and T2-weighted imaging with deep-learning reconstruction was 4 min and 16 s and 2 min and 12 s, respectively. The signal-to-noise ratio of the perirectal fat tissue and internal obturator muscle and contrast ratio of fat/muscle and bone/muscle determined via T2-weighted imaging with deep-learning reconstruction were significantly superior to those determined via conventional T2-weighted imaging (both  $p < 0.01$ ). Compared with conventional T2-weighted imaging, T2-weighted imaging with deep-learning reconstruction showed significant improvement in the visualization of the periprostatic anatomy, overall image quality, and motion artifacts (both  $p < 0.05$ ). Compared with conventional methods, T2-weighted imaging with deep-learning reconstruction facilitated the acquisition of good-quality magnetic resonance images of the prostate within a shorter acquisition time. T2-weighted imaging with deep-learning reconstruction will aid clinicians in diagnosing prostate cancer with shortened acquisition time while maintaining quantitative and qualitative image properties.

Keywords: deep learning, magnetic resonance imaging, prostatic cancer, signal-to-noise ratio, artifacts

#### Abbreviations:

C-T2: conventional T2-weighted imaging

DLR: deep-learning reconstruction

DL-T2: T2-weighted imaging with deep-learning reconstruction

MRI: magnetic resonance imaging

PI-RADS: Prostate Imaging Reporting and Data System

Received: July 31, 2024; accepted: September 30, 2024

Corresponding Author: Hayato Tomita, MD, PhD

Department of Radiology, St. Marianna University School of Medicine,

2-16-1 Sugao, Miyamae-ku, Kawasaki 216-8511, Japan

Tel: +81-44-977-8111, Fax: +81-44-977-2931, E-mail: hayato.tomita@marianna-u.ac.jp

SNR: signal-to-noise ratio

T2WI: T2-weighted imaging

This is an Open Access article distributed under the Creative Commons Attribution-NonCommercial-NoDerivatives 4.0 International License. To view the details of this license, please visit (<http://creativecommons.org/licenses/by-nc-nd/4.0/>).

## INTRODUCTION

Prostate cancer is the second most common cancer affecting men worldwide, accounting for 14.2% of all cases of cancer among men.<sup>1</sup> The diagnosis of prostate cancer is confirmed by measuring the prostate-specific antigen levels in the blood, transrectal ultrasonography, magnetic resonance imaging (MRI), and biopsy.<sup>2</sup>

A combined sequence of T2-weighted imaging (T2WI), diffusion-weighted imaging, and contrast-enhanced dynamic studies has been used for imaging prostate cancer lesions.<sup>3</sup> Presently, prostate MRI is performed in accordance with the Prostate Imaging Reporting and Data System (PI-RADS) Version 2.1.<sup>4</sup> This reduces variations in image interpretation among radiologists, stratifies patients according to risk, and aids in deciding whether biopsy or follow-up is the more suitable treatment choice. Prostate T2WI has been used to identify the anatomical structures and evaluate the PI-RADS score in the transitional zone. A technique that can shorten the acquisition time while maintaining the image quality of prostate T2WI would be useful in clinical practice.

The quality of the MR images plays a crucial role in the accurate diagnosis of prostate cancer. However, a trade-off relationship between image quality and the acquisition time of MRI has been observed: prioritizing image quality increases the acquisition time, which in turn increases motion artifacts.<sup>5</sup> Several sensing and reconstruction technologies have been applied to medical imaging to improve image quality and shorten the acquisition time.<sup>6-8</sup> Deep-learning reconstruction (DLR) has the potential to improve the acquisition time while maintaining the image quality by decreasing motion artifacts and removing noises.<sup>9</sup> Therefore, it was hypothesized that prostate T2WI with DLR (DL-T2) could improve the image quality and shorten the acquisition time compared with conventional T2WI (C-T2). This study thus aimed to clarify the superiority of prostate DL-T2 over C-T2 via quantitative and qualitative analyses.

## MATERIALS AND METHODS

This retrospective chart review study involving human participants was conducted in accordance with the ethical standards of the institutional and national research committee, and with the 1964 Helsinki Declaration and its later amendments or comparable ethical standards. This study was approved by the Ethics Committee of the St. Marianna University School of Medicine (approval number: 6123). The requirement for obtaining informed consent was waived owing to the retrospective nature of the study. Information on opt-out requests for refusal to participate in the study was disclosed on the institution's website.

### *Study patients*

Patients with suspected prostate cancer who had undergone prostate MR imaging, including DL-T2 and C-T2, between April 2022 and June 2023 were eligible for inclusion in this retrospective study. Patients who had received chemotherapy and those who had undergone prostate resection were excluded.

*MR protocols*

All patients underwent MR examinations performed using a 3T MRI system (Vantage Galan 3T; Canon Medical Systems Corporation, Tochigi, Japan). Table 1 presents the scan parameters. A DLR method based on the Advanced Intelligent Clear-IQ Engine (AiCE; Canon Medical Systems Corporation, Tochigi, Japan) was used in this study. The AiCE incorporates three parameters. The “Denoise Level” regulates sharpness in five levels, while the “AiCE Adjust” is similar to the denoising threshold and specifies the amount of denoising between 0.7 and 3.0. Finally, the “Edge Enhancement” determines whether edge enhancement processing is performed and is typically set to on. In this study, the parameters were configured as follows: Denoise Level = d02, AiCE Adjust = 1.4, and Edge Enhancement = on.

**Table 1** Magnetic resonance parameters of C-T2 and DL-T2

Parameters	C-T2	DL-T2
Acquisition time	2'12"	4'16"
Echo time (ms)	140	140
Repetition time (ms)	6900	6900
Acquisition matrix	256 × 288	256 × 288
Slice thickness (mm)	4.0	4.0
Number of signal averages	1	2
Parallel acquisition technique	SPEEDER	SPEEDER

C-T2: conventional T2-weighted imaging

DL-T2: T2-weighted imaging with deep-learning reconstruction

SPEEDER: parallel imaging technology installed in the Vantage Galan 3T (Canon Medical Systems Corporation, Tochigi, Japan)

*Quantitative image analysis*

Circular regions of interest (15–30 mm<sup>2</sup>) were placed on the regions containing perirectal fat tissue, internal obturator muscle, and pubic tubercle on the DL-T2 and C-T2 images to determine the signal intensity and standard deviation, respectively. The standard deviation of the region of interest in the tissue was used as the noise. The signal-to-noise ratio (SNR) and contrast ratio (CR) were calculated using the following equations:

$$SNR = \frac{SI}{SD} \quad (1)$$

$$CR = \frac{SI_{fp} - SI_m}{SI_m} \quad (2),$$

where SI<sub>fp</sub> denotes the signal intensity of the fat tissue or pubic tubercle, and SI<sub>m</sub> denotes the signal intensity of the obturator muscle. The CR was calculated by dividing the perirectal fat tissue and pubic tubercle by the internal obturator muscle.

*Qualitative image analysis*

The visualization of each anatomical structure (surgical capsule, anatomical capsule, anterior fibromuscular tissue, bladder prostate, rectal prostate, seminal vesicle, rectus pubis muscle, and internal obturator muscle) and overall image quality were evaluated by two diagnostic radiologists

with 4 and 12 years of experience in abdominal MR. The visualization of each structure was classified on a 5-point scale, with each score indicating the following: 1, not detectable; 2, poor (severe blurring); 3, fair (moderate blurring); 4, good (minimal blurring but all anatomical details retained); and 5, excellent (all anatomical details detectable without blurring). The overall image quality was classified on a 5-point scale, with each score indicating the following: 1, undiagnostic; 2, poor; 3, acceptable; 4, good; and 5, excellent. Motion artifacts were also classified on a 4-point scale, with each score indicating the following: 1, massive artifacts influencing diagnosis; 2, major artifacts influencing structure visualization; 3, minor artifacts that do not influence visualization of any structure; and 4, no detectable artifacts.

### Statistical analysis

The data were analyzed using JMP Pro version 16.2.0 (SAS Institute, NC, USA). Nonparametric data were analyzed using the Wilcoxon signed-rank test to determine the mean and  $p$ -value.  $P$ -values  $< 0.05$  were considered statistically significant. The intraclass correlation coefficients of qualitative image evaluations between the two radiologists were interpreted as follows:  $<0.5$ , poor;  $0.5$ – $0.7$ , moderate;  $0.7$ – $0.9$ , good;  $0.9$ – $1.0$ , excellent agreement.

## RESULTS

### Patient population

Among the 109 patients with suspected prostate cancer who underwent MR imaging, three patients who received chemotherapy and underwent surgery were excluded. Thus, 106 patients ( $71 \pm 8.3$  years; 106 men) with a median prostate-specific antigen level of 6.9 (interquartile range: 5.0–10.8) ng/mL were included in this study.

### Quantitative image analysis

Table 2 presents the results of the quantitative evaluations wherein intensity, standard deviation, and SNR were measured for the perirectal fat tissue, internal obturator muscle, and pubic tubercle. Except for the SNR of the pubic tubercle, the standard deviation and SNR measured via DL-T2 were significantly superior to those measured via C-T2, (both  $p < 0.01$ ). Significant differences were observed between C-T2 and DL-T2 in terms of the CR of fat-muscle and bone-muscle ( $p < 0.01$ ).

**Table 2** Comparison of quantitative image analysis results between C-T2 and DL-T2 for prostate magnetic resonance imaging

	C-T2 Mean $\pm$ SD	DL-T2 Mean $\pm$ SD	$p$ -value
Fat intensity	6608.3 $\pm$ 992.3	6839.3 $\pm$ 962.9	$<0.001$
Fat SD	274.2 $\pm$ 91.4	224.6 $\pm$ 76.2	$<0.001$
Fat SNR	26.8 $\pm$ 9.9	33.4 $\pm$ 11.0	$<0.001$
Muscle intensity	643.9 $\pm$ 145.4	625.5 $\pm$ 154.9	0.135
Muscle SD	236.9 $\pm$ 55.2	188.2 $\pm$ 41.8	$<0.001$
Muscle SNR	2.8 $\pm$ 0.9	3.5 $\pm$ 1.2	$<0.001$
PT intensity	4822.9 $\pm$ 1104.6	4854.9 $\pm$ 1180.5	0.001
PT SD	429.7 $\pm$ 138.9	445.2 $\pm$ 146.1	0.013

PT SNR	12.1 ± 3.7	11.7 ± 3.6	0.100
CR Fat-Muscle	10.1 ± 3.9	10.6 ± 4.2	<0.001
CR PT-Muscle	6.8 ± 2.3	7.3 ± 3.2	0.004

C-T2: conventional T2-weighted imaging

DL-T2: T2-weighted imaging with deep-learning reconstruction

PT: pubic tubercle

SD: standard deviation

SNR: signal-to-noise ratio

CR: contrast ratio

### Qualitative image analysis

Table 3 presents the results of the qualitative evaluation of each anatomical structure around the prostate, overall image quality, and motion artifacts using a 5- or 4-point scale. For both radiologists, DL-T2 was significantly higher than C-T2 in all quantitative analyses (both  $p < 0.05$ ). The intraclass correlation coefficient was calculated to determine the agreement between the readers. The intraclass correlation coefficient indicated good agreement between the radiologists (C-T2 = 0.848, DL-T2 = 0.778).

**Table 3** Comparison of qualitative image analysis results between C-T2 and DL-T2 for prostate magnetic resonance imaging

	Reader 1			Reader 2		
	Mean ± SD		<i>p</i> -value	Mean ± SD		<i>p</i> -value
	C-T2	DL-T2		C-T2	DL-T2	
Surgical capsule	4.4 ± 0.8	4.9 ± 0.4	<0.001	4.5 ± 0.7	4.8 ± 0.5	<0.001
Anatomical capsule	4.6 ± 0.7	4.9 ± 0.3	<0.001	4.6 ± 0.7	4.9 ± 0.4	<0.001
Anterior fibromuscular tissue	4.6 ± 0.7	4.9 ± 0.4	<0.001	4.7 ± 0.7	4.9 ± 0.4	<0.001
Bladder-prostate	4.6 ± 0.7	4.9 ± 0.4	<0.001	4.5 ± 0.7	4.8 ± 0.5	<0.001
Rectum-prostate	4.6 ± 0.7	4.9 ± 0.3	<0.001	4.6 ± 0.6	4.9 ± 0.3	<0.001
Seminal vesicle	4.5 ± 0.8	4.9 ± 0.3	<0.001	4.5 ± 0.8	4.7 ± 0.6	<0.001
Rectus pubis muscle	4.5 ± 0.5	5.0 ± 0.2	<0.001	4.8 ± 0.5	4.9 ± 0.4	<0.001
Internal obturator muscle	4.9 ± 0.3	5.0 ± 0.1	0.004	4.9 ± 0.4	4.9 ± 0.2	0.025
Overall image quality	4.5 ± 0.4	4.9 ± 0.2	<0.001	4.5 ± 0.7	4.9 ± 0.3	<0.001
Motion artifact	3.8 ± 0.5	3.9 ± 0.3	<0.001	3.8 ± 0.5	3.9 ± 0.3	<0.001

C-T2: conventional T2-weighted imaging

DL-T2: T2-weighted imaging with deep-learning reconstruction

SD: standard deviation

## DISCUSSION

The image quality of C-T2 and DL-T2 in prostate MR was evaluated in this study. Qualitative evaluation revealed that the SNR and CR of DL-T2 were significantly higher than those of C-T2. Moreover, DL-T2 achieved superior visibility, and the acquisition time of DL-T2 was approximately half of that of C-T2. Thus, DL-T2 can shorten the acquisition time while maintaining the quantitative and qualitative properties of the image, indicating that it may be useful in clinical practice.

MRI plays an important role in diagnosing prostate cancer. Improving the quality of MR images for prostate cancer will facilitate accurate diagnosis; however, there is a trade-off between image quality and acquisition time. Reducing the pixel size to improve image quality results in a reduction in signal intensity; consequently, increasing the number of signal averages is necessary. This results in an increase in acquisition time and motion artifacts (which are also increased by patient factors).<sup>5</sup> The use of PI-RADS for prostate imaging has enabled clinicians to make a diagnosis according to certain criteria; however, noise and artifacts must be minimized to maximize the effectiveness of PI-RADS. MR technologies, such as parallel imaging and compressed sensing, have been used to reduce the imaging time in the domain of prostate MRI.<sup>10</sup> Reconstruction techniques using artificial intelligence that can be applied to medical imaging have been actively studied in recent years. Ueda et al reported that DLR improved the image quality and the ability to differentiate malignant and benign prostate lesions on diffusion-weighted images.<sup>11</sup> Although several studies have applied DLR to prostate MRI, they differ in terms of vendors, parameters, and number of patients.<sup>9,12-16</sup> The DLR mechanism can be described as follows. Ideal high-resolution images are first obtained from several participants during the training process. These images were mixed with noise using a neural network to obtain low-noise images. The resulting images were compared with native images subsequently. The algorithm was modified and the denoising process was repeated if differences were observed. A learned database was created in this manner. The system can distinguish the signal from noise on the noisy raw data, perform noise removal using an algorithm, and create denoised images

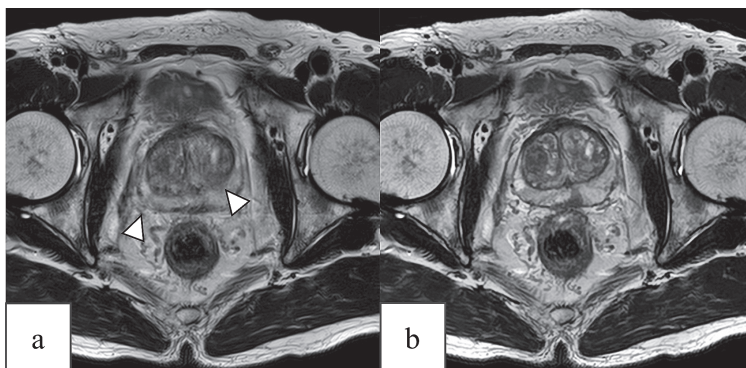


**Fig. 1** Prostate images of a 76-year-old man with suspected prostate cancer and prostate-specific antigen levels of 9.08 ng/mL

**Fig. 1a:** Conventional T2-weighted imaging

**Fig. 1b:** T2-weighted imaging with deep-learning reconstruction

The surgical and anatomical capsules in T2-weighted imaging with deep-learning reconstruction were more recognizable than those in conventional T2-weighted imaging (arrowheads). The overall blurring was reduced in T2-weighted imaging with deep-learning reconstruction.

in clinical practice. The implementation of this technique has resulted in a shorter acquisition time and higher spatial resolution compared with those of conventional reconstruction.<sup>17,18</sup> The acquisition time for C-T2 and DL-T2 was 4 min 16 s and 2 min 12 s, respectively. The number of signal averages for C-T2 and DL-T2 was 2 and 1, respectively. Although this technique was very effective in suppressing motion artifacts, DL-T2 can achieve a higher SNR than C-T2. The DLR used in the present study was characterized by the ability to increase the SNR, and the results were consistent with this ability. In addition, the image quality achieved by DL-T2 for each anatomical structure and motion artifact was better than that of C-T2. Figure 1 shows an example of easily recognizable changes in C-T2 and DL-T2 in the same case. The image acquired using DL-T2 showed fewer motion artifacts and good contrast of fine structures, partly owing to the denoising technique and the suppression of body motion due to the reduction in the imaging time facilitated by DLR.

Nevertheless, this study has some limitations. First, although DL-T2 was examined using the parameters recommended by the PI-RADS, each parameter of DLR could not be defined completely. Second, as this was a single-center study, the findings must be considered only after unifying the parameters among multiple institutions. Third, the clinical application of the DLR is not established at present. The accuracy of DL improves as the amount of data increases; thus, improved DLR models may be produced and introduced in the future. Fourth, the effect of DL-T2 on PI-RADS scores was not examined in this study. The evaluation of the surgical and anatomical capsules of the prostate showed significant differences in the visualization of capsular structures. However, there has yet to be an evaluation on the visualization and contour of the tumor according to PIRADS. Accurate contrast with pathology is preferable for optimal tumor diagnostic performance, but few biopsy cases were available at the time of this study. In future research, we will focus exclusively on patients with tumors, analyzing the visualization and contour of the tumor and its impact on the PIRADS score, along with the pathology results.

In conclusion, T2WI using DLR can improve the qualitative and quantitative properties of prostate MR images within a shorter acquisition time.

## AUTHOR CONTRIBUTIONS

DK performed data curation, formal analysis, investigation and writing-original draft. HT supported conceptualization, investigation and administration. YK and HM supervised this project. All authors have conformed this manuscript and provided advices.

## FINANCIAL SUPPORT

No funding was received for this study.

## CONFLICT OF INTEREST

The authors have no conflict of interest to disclose.

## DATA AVAILABILITY

Data supporting the findings of this study are available from the corresponding author on request.

## REFERENCES

- 1 International Agency for Research on Cancer, World Health Organization. Factsheets. Published February 2024. Accessed July 28, 2024. <https://gco.iarc.fr/today>
- 2 Sekhoacha M, Riet K, Motloung P, Gumenuk L, Adegoke A, Mashele S. Prostate cancer review: Genetics, diagnosis, treatment options, and alternative approaches. *Molecules*. 2022;27(17):5730. doi:10.3390/molecules27175730
- 3 Penzkofer T, Tempny-Afdhal CM. Prostate cancer detection and diagnosis: The role of MR and its comparison with other diagnostic modalities – A radiologist’s perspective. *NMR Biomed*. 2014;27(1):3–15. doi:10.1002/nbm.3002
- 4 Turkbey B, Rosenkrantz AB, Haider MA, et al. Prostate imaging reporting and data system version 2.1: 2019 update of prostate imaging reporting and data system version 2. *Eur Urol*. 2019;76(3):340–351. doi:10.1016/j.eururo.2019.02.033
- 5 Obuchowicz R, Piórkowski A, Urbanik A, Strzelecki M. Influence of acquisition time on MR image quality estimated with nonparametric measures based on texture features. *BioMed Res Int*. 2019;2019:3706581. doi:10.1155/2019/3706581
- 6 Tomita H, Deguchi Y, Fukuchi H, et al. Combination of compressed sensing and parallel imaging for T2-weighted imaging of the oral cavity in healthy volunteers: Comparison with parallel imaging. *Eur Radiol*. 2021;31(8):6305–6311. doi:10.1007/s00330-021-07699-y
- 7 Cristobal-Huerta A, Poot DHJ, Vogel MW, Krestin GP, Hernandez-Tamames JA. Compressed sensing 3D-GRASE for faster high-resolution MRI. *Magn Reson Med*. 2019;82(3):984–999. doi:10.1002/mrm.27789
- 8 Ouchi S, Ito S. Reconstruction of compressed-sensing MR imaging using deep residual learning in the image domain. *Magn Reson Med Sci*. 2021;20(2):190–203. doi:10.2463/mrms.mp.2019-0139
- 9 Gassenmaier S, Afat S, Nickel D, Mostapha M, Herrmann J, Othman AE. Deep learning-accelerated T2-weighted imaging of the prostate: Reduction of acquisition time and improvement of image quality. *Eur J Radiol*. 2021;137:109600. doi:10.1016/j.ejrad.2021.109600
- 10 Tsao J, Kozerke S. MRI temporal acceleration techniques. *J Magn Reson Imaging*. 2012;36(3):543–560. doi:10.1002/jmri.23640
- 11 Ueda T, Ohno Y, Yamamoto K, et al. Deep learning reconstruction of diffusion-weighted MRI improves image quality for prostatic imaging. *Radiology*. 2022;303(2):373–381. doi:10.1148/radiol.204097
- 12 Roest C, Fransen SJ, Kwee TC, Yakar D. Comparative performance of deep learning and radiologists for the diagnosis and localization of clinically significant prostate cancer at MRI: A systematic review. *Life (Basel)*. 2022;12(10):1490. doi:10.3390/life12101490
- 13 Schelb P, Tavakoli AA, Tubtawee T, et al. Comparison of prostate MRI lesion segmentation agreement between multiple radiologists and a fully automatic deep learning system. *Rofo*. 2021;193(5):559–573. doi:10.1055/a-1290-8070
- 14 Schelb P, Wang X, Radtke JP, et al. Simulated clinical deployment of fully automatic deep learning for clinical prostate MRI assessment. *Eur Radiol*. 2021;31(1):302–313. doi:10.1007/s00330-020-07086-z
- 15 Gassenmaier S, Afat S, Nickel MD, et al. Accelerated T2-weighted TSE imaging of the prostate using deep learning image reconstruction: A prospective comparison with standard T2-weighted TSE imaging. *Cancers (Basel)*. 2021;13(14):3593. doi:10.3390/cancers13143593
- 16 Kim EH, Choi MH, Lee YJ, Han D, Mostapha M, Nickel D. Deep learning-accelerated T2-weighted imaging of the prostate: Impact of further acceleration with lower spatial resolution on image quality. *Eur J Radiol*. 2021;145:110012. doi:10.1016/j.ejrad.2021.110012
- 17 Kidoh M, Shinoda K, Kitajima M, et al. Deep learning based noise reduction for brain MR imaging: Tests on phantoms and healthy volunteers. *Magn Reson Med Sci*. 2020;19(3):195–206. doi:10.2463/mrms.mp.2019-0018
- 18 Tajima T, Akai H, Sugawara H, et al. Breath-hold 3D magnetic resonance cholangiopancreatography at 1.5 T using a deep learning-based noise-reduction approach: Comparison with the conventional respiratory-triggered technique. *Eur J Radiol*. 2021;144:109994. doi:10.1016/j.ejrad.2021.109994